Titles: Isolating and reconstructing key components of North Atlantic Ocean variability from a sclerochronological spatial network

Authors:

Reynolds D.J.[1]*, Hall, I.R.[1], Slater, S.M.[1], Mette, M.[2], Wanamaker, A.D.[2], Scourse, J.D.[3], Garry, F.K.[4], and Halloran, P.R.[4]

Authors contact details:

[1]School of Earth and Ocean Sciences, Cardiff University, Park Place, Cardiff, CF10 3AT, UK.

[2]Department of Geological and Atmospheric Sciences, Iowa State University, Ames, Iowa, 50011-3212, USA.

[3]College of Life and Environmental Sciences, University of Exeter, Penryn Campus, Penryn, TR10 9EZ, UK.

[4] College of Life and Environmental Sciences, Exeter University, Rennes Drive, Exeter, EX4 4RJ, UK.

Abstract

Our understanding of North Atlantic Ocean variability within the coupled climate system is limited by the brevity of instrumental records and a deficiency of absolutely dated marine proxies. Here we demonstrate that a spatial network of marine stable oxygen isotope series derived from molluscan sclerochronologies ($\delta^{18}O_{shell}$) can provide skillful annually resolved reconstructions of key components of North Atlantic Ocean variability with absolute dating precision. Analyses of the common $\delta^{18}O_{shell}$ variability, using principal component analyses (PCA), highlight strong connections with tropical North Atlantic and subpolar gyre (SPG) sea surface temperatures (SSTs) and sea surface salinity (SSS) in the North Atlantic Current (NAC) region. These analyses suggest that low frequency variability is dominated by the tropical Atlantic signal whilst decadal variability is dominated by variability in the SPG and salinity transport in the NAC. Split calibration and verification statistics indicate that the composite series produced using the PCA can provide skillful quantitative reconstructions of tropical North Atlantic and SPG SSTs and NAC SSSs over the industrial period (1864-2000). The application of these techniques with extended individual $\delta^{18}O_{shell}$ series provide powerful baseline records of past North Atlantic variability into the unobserved pre-industrial period. Such records are essential for developing our understanding of natural climate variability in the North Atlantic Ocean and the role it plays in the wider climate system, especially on multi-decadal to centennial timescales, potentially enabling reduction of uncertainties in future climate predictions.

Main Text

Our understanding of past North Atlantic circulation dynamics and the influence these changes have on the wider climate system are limited both by the short temporal and limited spatial distribution of marine observations, as well as by the large uncertainties typical of proxy reconstructions dated using radiocarbon-derived age models (typically ±100 years). Whilst sediment core records provide invaluable baseline records of past marine variability, their associated age model uncertainties preclude the analysis of multiple cores to resolve decadal or sub-decadal scale changes in the spatial patterns of marine variability. Spatial networking techniques have facilitated the reconstruction of regional to hemispheric-scale modes (i.e., patterns) of atmospheric variability based on the analysis of suites of absolutely-dated, via band counting and crossdating, tree ring series (dendrochronologies; e.g. (Moberg et al., 2005, Wilson et al., 2016). The precisely-dated nature of the dendrochronologies, based on crossdating (Black et al., 2016), enables the assessment of the absolute timing of variability between these climate records constructed across broad geographical regions; local changes affecting single proxy records are "averaged out" allowing the common variability across the network to be identified (Wilson et al., 2010). While such techniques have been extensively used in terrestrial paleoclimatology, the lack of absolutely-dated and annually-resolved marine climate records has precluded this approach being widely used in the marine environment. Currently, in the extra-tropical North Atlantic, investigations of marine proxy networks have been limited to the evaluation of low frequency (centennial) ocean variability (e.g. Cunningham et al., 2013, McGregor et al., 2015), with high frequency (decadal/sub-decadal) marine variability being derived through extrapolation of terrestrial proxy networks, largely dendrochronologies, on adjacent landmasses (e.g. Gray, 2004, Mann et al., 2009, Rahmstorf et al., 2015). It is important to note that the application of these terrestrial tree ring proxy networks to derive an ocean climate field reconstruction prevents the independent examination of the influence that marine variability has on, for example, Northern Hemispheric surface air temperatures (NHSAT), as the reconstructions of NHSAT incorporate the same tree ring records.

Here we demonstrate the potential for utilizing a spatial network of precisely-dated marine molluscan stable oxygen isotope ($\delta^{18}O_{shell}$) series to reconstruct inter-annual to multi-decadal variability in the North Atlantic Ocean over the industrial era. Molluscan sclerochronologies, a marine counterpart to dendrochronologies, provide a basis for the direct application of spatial networking techniques given their absolutely-dated and annually-resolved nature. In recent years, absolutely-dated $\delta^{18}O_{shell}$ records have been developed from sites located in Scotland (Reynolds et al., 2017a), Norway (Mette et al., 2016), Iceland (Reynolds et al., 2016) and the Gulf of Maine (Wanamaker et al., 2008). These records, based on the $\delta^{18}O$ analysis of carbonate samples derived from the crossdated annual growth increments of the long-lived bivalve molluscs *Arctica islandica* and *Glycymeris glycymeris,* each demonstrate significant sensitivity to broad scale North Atlantic Ocean variability. Whilst these four independent records represent a seemingly small marine proxy network relative to the abundance of records included in dendrochronological-derived spatial networks, observation-based analysis at the four sampling locations supports their value in reconstructing broad scale North Atlantic variability.

This study therefore sets out to 1: investigate the potential of generating statistically significant composite series using principal component analysis (PCA) on multiple $\delta^{18}O_{shell}$ series from the continental shelf seas of the North Atlantic; 2: investigate the sensitivity of the resulting composite series to broad scale variability in SSTs and SSSs in the North Atlantic Ocean; 3: quantitatively evaluate the skill of the composite series at reconstructing components of North Atlantic variability. Our proof of concept approach used here will enable future workers to apply similar statistical techniques as more sclerochronological records become available.

Methodology

Sampling locations and Individual $\delta^{18}O_{shell}$ series

In this study we utilize four independently constructed $\delta^{18}O_{shell}$ series derived from the annually-resolved shell growth increments of the long-lived marine bivalve molluscs *Arctica islandica* and *Glycymeris glycymeris* (Supplementary Table 1). The four independent $\delta^{18}O_{shell}$ series were constructed by analyzing the oxygen isotope composition of annual growth increments from shell material that was collected from the shelf seas off the coasts of Scotland, Gulf of Maine (USA), North Iceland and North Norway (Figure 1 and Supplementary Table 1). The shells were collected from 6-80 m water depth. The individual $\delta^{18}O_{shell}$ series span a range of time intervals with the shortest spanning the 20th century (Norway; Mette et al., 2016) and the longest spanning the entirety of the last millennium (North Iceland; Reynolds et al., 2016). Preliminary analyses of the covariance between the four records was conducted using linear regression analyses over the record's coeval period of 1900-2000. The significance of the regressions was tested using the Ebisuzaki Monte Carlo methodology to take account for auto-correlation contained in each of the time series (Ebisuzaki, 1997). The $\delta^{18}O_{shell}$ data from each series are shown in Supplementary Figure S1.

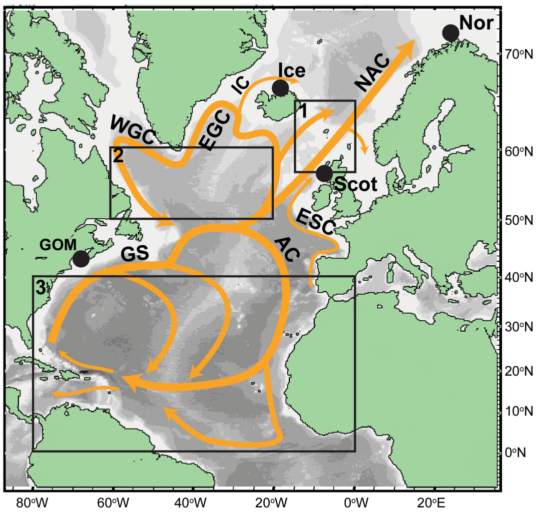

Figure 1: A schematic of the North Atlantic Ocean surface currents (orange arrows) and the sampling localities (black circles) of stable oxygen isotope series used to construct the $\delta^{18}O_{PC1\text{-}S1\text{-}S3}$ composite. Ice = Iceland; Nor = Norway; Scot = Scotland; GOM = Gulf of Maine; NAC = North Atlantic Current; GS = Gulf Stream; EGC = East Greenland Current; WGC = West Greenland Current; ESC = European Slope Current; IC = Irminger Current; AC = Azores Current. Black boxes 1-3 denote the regions from which SST and SSS were obtained from the HadISST1 and EN4 SSS gridded data sets for the environmental analyses. Box 1 represents North Atlantic Current waters; box 2 broadly represents the North Atlantic subpolar gyre; and box 3 represents the tropical North Atlantic. Bathymetry data provided by Global Bathymetric Chart of the Oceans (GEBCO; https://www.gebco.net) plotted in GeoMapApp (www.geomapapp.org). Ocean circulation modified from Marzocchi et al. (2015).

Spatial network construction and validation

To extract the common variability recorded across the four individual $\delta^{18}O_{shell}$ series we used a nested PCA approach (Wilson et al., 2010, Cunningham et al., 2013). To evaluate the possible influence of variable (non-stationary) coherence between the four locations that may occur in response to, for example, changes in atmospheric and/or ocean circulation patterns over the wider North Atlantic region, the PCA analyses were conducted using three differing strategies. Strategy 1 was a conventional nested PCA using the longest period of overlap between the four series (1900-2000) with the resulting principal component (PC) providing the primary nest. The shortest independent $\delta^{18}O_{shell}$ series (Norway) was then removed and the PCA repeated using the remaining three independent $\delta^{18}O_{shell}$ series for their coeval period. The resulting PC provided the secondary nest (1864-2000). The interval of the secondary nest not represented in the primary nest (1864-1899) was then combined, with no overlap, to provide a final strategy 1 composite series (1864-2000). In strategy 2, the four independent $\delta^{18}O_{shell}$ series were split into three non-overlapping bins with periods spanning 1901-1950, 1951-2000 (containing all four series) and 1864-1900 (containing the three longest series, i.e. Norway removed) respectively. PCA was then conducted on the three bins independently, generating PCs for each time period. The PCs from each bin were then combined with no period of overlap to create a final strategy 2 composite series that spans 1864-2000. In the last approach, Strategy 3, the four independent $\delta^{18}O_{shell}$ series were split into 30 year bins, with each bin overlapping by 20 years. The PCA was then conducted on each 30 year bin and the PCs combined by arithmetically averaging the overlapping years to create a final strategy 3 composite series that spans 1864-2000. Strategies two and three were adopted as they provided at least three bins across the 1864-2000 period with sufficient data to conduct the PCA (i.e. at least three independent $\delta^{18}O_{shell}$ series and ≥30 years duration). In each strategy a minimum of three independent $\delta^{18}O_{shell}$ series contributed to the resulting composite series throughout the 1864-2000 period. Eigenvalue and percentage variance statistics were used to evaluate the significance of the PCs produced across all nests using each PCA strategy. Nests that contained Eigenvalues <1 were omitted from the final composite series. The primary PCs extracted from the three PCA strategies are referred to hereafter as $\delta^{18}O_{PC1\text{-}S1}$, $\delta^{18}O_{PC1\text{-}S2}$ and $\delta^{18}O_{PC1\text{-}S3}$ respectively and collectively referred to as $\delta^{18}O_{PC1\text{-}S1\text{-}3}$. The second PCs produced are referred to as $\delta^{18}O_{PC2\text{-}S1}$ and $\delta^{18}O_{PC2\text{-}S2}$ respectively. Due to a lack of significance (Eigenvalues <1) no tertiary PC's were extracted using strategies 1 and 2 and no secondary or tertiary PC's were extracted using strategy 3. PCAs were conducted using SBSS statistics v20 and PAST V3.18. Supplementary Figure S2 shows a schematic diagram representing the construction of each of the three strategies, the time interval represented by each of the nests and the respective $\delta^{18}O_{shell}$ series each nest contains.

It is important to note that recalculating the PCA across multiple bins and then combining the resulting PCs (as in strategies 2 and 3) acts to remove the low frequency variability (effectively acting as a high pass filter) due to the data normalization required in the calculation of the PCA in each bin. As a result, the $\delta^{18}O_{PC1\text{-}S2}$ and $\delta^{18}O_{PC1\text{-}S3}$ series only contain variability on timescales <50 and <30 years respectively. Therefore, to assess the influence our binning strategy might have had on the resulting composite series, the PCA was repeated, using strategy 1, but based on independent $\delta^{18}O_{shell}$ data initially treated using a range of first order loess high pass filter ranging between 10 to 200 years respectively. The resulting composite records generated, which each span the 1900-2000 interval and contain all four individual $\delta^{18}O_{shell}$ records, are referred to as $\delta^{18}O_{PC1\text{-}F}$.

Evaluating the influence of the number of proxy series in the spatial network

Given the relatively low number of independent $\delta^{18}O_{shell}$ series utilized it is important to assess the sensitivity of the composite $\delta^{18}O_{PC1\text{-}S1\text{-}3}$ series to potential biases associated with an individual $\delta^{18}O_{shell}$ series. To do this, the strategy 1 PCA was repeated with the omission of one individual $\delta^{18}O_{shell}$ series (Supplementary Table 3). The PCA was replicated an additional four times, each time omitting a different independent $\delta^{18}O_{shell}$ series, but always containing at least three $\delta^{18}O_{shell}$ series. In total this approach generated five primary PCs, one containing all four independent $\delta^{18}O_{shell}$ series and four composites containing three independent $\delta^{18}O_{shell}$ series, each spanning the interval from 1900-2000. The PCA statistics and linear regression analyses, evaluated using the Ebisuzaki Monte Carlo methodology, conducted between each of the primary PCs, were then used to evaluate the relative influence of the independent $\delta^{18}O_{shell}$ series on the $\delta^{18}O_{PC1\text{-}S1}$ series (Supplementary Figure S3 and Supplementary Table 3).

The $\delta^{18}O_{PC1\text{-}S1\text{-}3}$ series were compared with pseudo primary PCs derived using PCA on the gridded SST, SSS data products and the predicted $\delta^{18}O$ composition of aragonite ($\delta^{18}O_{syn}$) at each of the four locations for the period 1900-2000. The PCA was conducted using SST (HadISST1; Rayner et al., 2003) and SSS (EN4 SSS; Good et al., 2013) data derived from 2x2° grid boxes from each of the four sampling locations and the primary PCs extracted (referred to hereafter as SST_{PC1} and SSS_{PC1} (Figure 3 and

Supplementary Figure S6). Whilst there are uncertainties associated with gridded data products, associated with the reduced number of observations during the early half of the 20th century (Supplementary Figure S4), these pseudo data still provide a useful test of the skill of the composite series at capturing the long-term variability in the North Atlantic system. Replication of these analyses using different gridded data products (e.g. ER SST V3 (Smith et al., 2008), ICOADs (Freeman et al., 2017) and HadSST3 (Kennedy et al., 2011) suggests the results are consistent regardless of the data product used (Supplementary Figure S5). The $\delta^{18}O_{syn}$ data were generated using the Grossman and Ku (1986) aragonite palaeotemperature equation coupled with the local salinity mixing line equations at each of the four sites (Smith et al., 2005, Cage and Austin, 2010, Mette et al., 2016, Whitney et al., 2017) to convert from local SST and SSS data to $\delta^{18}O_{syn}$. PCA was then conducted, using all three strategies, on the four independent $\delta^{18}O_{syn}$ records to derive the $\delta^{18}O_{syn-PC1-S1-3}$ composite records. These instrumental composites (SST_{PC1}, SSS_{PC1} and $\delta^{18}O_{syn-PC1-s1-3}$), spanning 1900-2000, were correlated against the coeval $\delta^{18}O_{PC1-S1-3}$ series, and the significance tested using the Ebisuzaki Monte Carlo methodology, to evaluate the relative influence of SST and SSS on the $\delta^{18}O_{PC1-S1}$ series.

As the bivalve molluscs lived (and recorded environmental conditions) at their collection water depths between 6-80 m water, an additional suite of composite series was generated to assess any potential differences in the comparison with observational sea surface parameters. As no instrumental measurements of bottom water temperature (or salinity) data are available at the four sampling locations, we conducted the PCA, using all three strategies, based on modelled bottom water temperatures at each site. The bottom water temperature data were obtained from an adaption of a 1D physical-biogeochemical model S2P3-R (v1.0) (Marsh et al., 2015) driven by National Centre for Environmental Prediction meteorology (http://www.ncep.noaa.gov/) and Oregon Tidal Prediction Software (http://volkov.oce.orst.edu/tides/otps.html) using bathymetry derived from the ETOP01 Earth topography model (https://www.ngdc.noaa.gov/mgg/global). The resulting PCs were correlated against the respective $\delta^{18}O_{PC1-s1-3}$ series and the significance of the correlations tested (Figure 3). Bottom water salinity was not included in this analysis.

Finally, given the shallow depth and habitat restriction to continental shelf seas of the long-lived marine bivalves used in our reconstructions, we examine the potential influence of including only a limited number of $\delta^{18}O_{shell}$ series from such regions in our spatial network. We constructed a purely 'hypothetical' spatial network using SST data derived from up to 25 independent 5°x5° grid boxes in the HadISST1 dataset from across the North Atlantic region (Supplementary Figure S9). Sites included in the hypothetical proxy network were 1) constrained to the continental margins (14 sites), to simulate the inclusion of additional sclerochronological records that can only be constructed in shelf sea locations, and 2) across the entire North Atlantic Ocean (25 sites; Supplementary Figure S9), to simulate a multi-proxy approach that could include the addition of high-resolution sediment core records. The resulting hypothetical composites were then correlated against mean North Atlantic SSTs over the 20th century to evaluate whether increasing the spatial coverage (and number) of records significantly improved the skill of the resulting network. Only SST data were used for these analyses due to a lack of salinity mixing line equations from across the entire study area. As no proxy is a perfect record of SST, clearly using instrumental data to simulate these theoretical reconstructions will likely lead to an overestimate of the absolute skill of the resulting composite series. However, these analyses do provide an indication of whether increasing the number of proxy series would result in an overall increase in skill of the resulting network.

Environmental analyses and reconstruction skill

To evaluate the sensitivity of the proxy and instrumental based composite series to North Atlantic marine variability, the $\delta^{18}O_{PC1-S1-3}$, $\delta^{18}O_{PC2-S1-2}$, SST_{PC1}, SSS_{PC1} and $\delta^{18}O_{syn\_PC1}$ series were correlated against gridded SST (HadISST1; Rayner et al., 2003) and SSS (EN4 SSS; Good et al., 2013) datasets over the North Atlantic region using point correlation analyses. The point correlations were conducted using both raw (un-detrended) and linear detrended annually averaged data over the 20th century using the KNMI Climate Explorer (Figure 4; Trouet and Van Oldenborgh, 2013). To provide a quantitative assessment of the identified spatial sensitivities, monthly SST and SSS data were obtained from the HadISST1 and EN4 SSS datasets for the tropical North Atlantic (0-40°N by 0-80°W), subpolar gyre (SPG; 50-60°N by 20-60°W) regions and between northern Scotland and the Faroe Isles (57-67°N by 0-10°W) to broadly reflect the northern trajectory of the NAC. Linear regression analyses were then performed between the composite series and the mean monthly, annual mean and seasonal mean SSTs and SSSs over the three regions (tropical North Atlantic, SPG and NAC; Figure 5 and Supplementary Figure S7).

A split calibration and verification statistical approach was used to calibrate the $\delta^{18}O_{PC1-S1-3}$ and $\delta^{18}O_{PC2-S1-2}$ series against the target SST and SSS timeseries and to evaluate the level of skill the calibrated timeseries has in reconstructing the target parameter (North, 2000). The calibration was generated using linear regression analyses between the $\delta^{18}O_{PC1-S1-3}$ and $\delta^{18}O_{PC2-S1-2}$ series and the target parameters, tropical North Atlantic SSTs [HadISST1], SPG SSTs [HadISST1] and NAC SSSs [EN4 SSS], over the period containing the strongest correlation (either 1900-1949 or 1950-2000 respectively). The portion of the gridded data not used for the calibration therefore remained independent and was used to verify and estimate the skill of the final reconstruction. The calibration was then applied to convert the full length $\delta^{18}O_{PC1-S1-3}$ and $\delta^{18}O_{PC2-S1-2}$ series to SSTs and SSSs. Whilst gridded data products spanning the early half of the 20th century contain increased uncertainty, these data still provide a useful indication of the ability of the calibrated reconstruction to track the long-term changes in SST and SSS variability over this region. Mean squared errors (MSE) were calculated between the calibrated $\delta^{18}O_{PC1-S1-3}$ series and the target parameters over both the calibration and verification periods, and reduction of error (RE) and coefficient of efficiency (CE) statistics calculated using the Ebisuzaki Monte Carlo methodology (Macias-Fauria et al., 2012). The calibration and verification statistics were estimated using the ReconStats package in Matlab R2015a (Macias-Fauria et al., 2012).

Multiple linear regression analyses were used to examine the total percentage variance that the SPG and tropical North Atlantic SST explain in the $\delta^{18}O_{PC1-S1}$ series. These analyses were conducted using R V3.4.1.

Assessing the sensitivity to North Atlantic circulation dynamics

As the $\delta^{18}O_{PC1-S1-3}$ and $\delta^{18}O_{PC2-1}$ series do not overlap with the RAPID observational record of North Atlantic transport at 26.5°N (Smeed et al., 2016), and only by a few years with the SPG index (Hatun et al., 2005), it is not possible to directly evaluate the covariance between direct measurements of North Atlantic circulation dynamics and the $\delta^{18}O_{PC1-S1-3}$/ $\delta^{18}O_{PC2-S1}$ series. We therefore analyzed the $\delta^{18}O_{PC1-S1-3}$ and $\delta^{18}O_{PC2-1}$ series against a tide-gauge based reconstruction of European Slope Current strength (ESC annual index, Marsh et al., 2017). The strength of the ESC is associated with both Ekman transport and seawater density gradients (Huthnance, 1984) and is positively linked with both changes in SPG and Atlantic Meridional Overturning Circulation (AMOC) strength (Marsh et al., 2017). The $\delta^{18}O_{PC1-S1-3}$ and $\delta^{18}O_{PC2-1}$ series were correlated against the ESC annual index using linear regression analyses over the interval from 1957-2000. These analyses were conducted using linear detrended data to remove the influence of long-term atmospheric warming not associated with changes in ESC strength.

To evaluate the influence of atmospheric circulation patterns on driving the variability in the proxy composite series, the proxy composite series were correlated against gridded sea level pressure (SLP (Trenberth and Paolino, 1980) and zonal wind stress datasets (20th century reanalysis V2 data acquired from the NOAA/OAR/ESRL PSD available at www.esrl.noaa.gov/psd/) over the 20th century. The correlations were calculated using the KNMI Climate Explorer Facility (Supplementary Figure 10).

Results and Discussion

Spatial network construction

Despite the large distances between each of the sampling locations significant, albeit weak, Pearson correlations were identified between the four independent $\delta^{18}O_{shell}$ series (e.g., R=0.30 P<0.1; and R=0.37 P<0.05 calculated between the Scottish and Gulf of Maine series and between the Iceland and the Gulf of Maine $\delta^{18}O_{shell}$ series; Supplementary Figure S1 and Supplementary Table 2). Despite the relatively weak correlations identified between the four independent $\delta^{18}O_{shell}$ series, the nested PCA resulted in the generation of significant (Eigenvalues >1) primary PCs using all three PCA strategies for the full period of 1864-2000 and the generation of significant secondary PCs using strategies 1 and 2 (Figure 2). The $\delta^{18}O_{PC2\text{-}S1\text{-}2}$ series were only significant over the period represented by all four individual $\delta^{18}O_{shell}$ series (1900-2000). Comparison of the replicated proxy composite series generated using PCA of different combinations of three out of the four independent $\delta^{18}O_{shell}$ series identified significant correlations between the resulting PCs (R=0.74-0.97; Supplementary Table S3 and supplementary Figure S3) and consistently high eigenvalues (1.41-1.73) and percentage variance statistics (43.6-55.1%). This result implies that there is no strong bias in the resulting composite series towards any of the four independent $\delta^{18}O_{shell}$ series. The identification of coherence between the four independent $\delta^{18}O_{shell}$ series, and generation of significant PCs (i.e. composite series), despite the large distances between the four locations, suggests a suite of common environmental mechanisms are likely driving variability across the four sampling localities (Cunningham et al., 2013, Wilson et al., 2016). Such a result is perhaps not surprising given the previously identified connectivity of the hydrographic settings of the four sampling locations to wider North Atlantic Ocean variability (Wanamaker et al., 2008, Wanamaker et al., 2011, Mette et al., 2016, Reynolds et al., 2016, Reynolds et al., 2017a).

The application of the PCA, using all three strategies, on the instrumental SST, SSS, $\delta^{18}O_{syn}$ data and model derived bottom water temperature data generated PCs with significant eigenvalues (>1). However, whilst the PCA of the $\delta^{18}O_{syn}$ data generated a robust PC1, using strategy 1, the eigenvalues for PC2 were <1 and therefore the $\delta^{18}O_{syn\text{-}PC2}$ data were not utilized in any further analyses. Linear regression analyses identified significant coherence between the $\delta^{18}O_{PC1\text{-}S1}$ series and the composites generated using instrumental SST and $\delta^{18}O_{syn}$ (SST_{PC1} R=-0.50, P<0.05 and $\delta^{18}O_{syn\text{-}PC1}$ R=0.55, P<0.05; calculated over the 20th century; Supplementary Figure S6). No significant correlation was identified between the $\delta^{18}O_{PC1\text{-}S1}$ series and the composite derived using SSS across the four sampling locations (SSS_{PC1} R=-0.37 P=0.18; Supplementary Figure S6). These results suggest that SST variability at the sampling locations dominates the variability in the $\delta^{18}O_{PC1\text{-}3}$ series. However, taking both SST and SSS variability into account (using the $\delta^{18}O_{syn\text{-}PC1}$ record) leads to a marginal improvement of the sensitivity of the proxy composite series to environmental variability.

The comparison of the proxy derived composites ($\delta^{18}O_{PC1\text{-}S1\text{-}3}$) against the $\delta^{18}O_{syn}$ and model derived composites highlights that the proxy composite series are, with the exception of the $\delta^{18}O_{PC1\text{-}S3}$ and $\delta^{18}O_{syn\text{-}S3}$ series, significantly coherent (P<0.1) with the variability contained in the instrumental and model based composite series (Figure 3). Whilst the $\delta^{18}O_{PC1\text{-}S3}$ and $\delta^{18}O_{syn\text{-}S3}$ series exhibit no significant coherence, the $\delta^{18}O_{PC1\text{-}S3}$ series and corresponding model derived composite series do significantly correlate (R-=0.40 P<0.05; Figure 3). Given that the Eigenvalue and percentage variance statistics for these series are significant, it is unlikely that the resulting composite series contain significant non-environmentally driven variability. We therefore suggest that the lack of coherence between the $\delta^{18}O_{PC1\text{-}S3}$ and $\delta^{18}O_{syn\text{-}S3}$ series stems from differences in temperature and salinity variability between sea surface and bottom water conditions at the sampling sites. Whilst the gridded data products used to generate the pseudo proxy network are a measure of surface water conditions, the shells used to generate the proxy network were collected at a range of water depths between 6-80m. Comparison of the proxy derived composite $\delta^{18}O_{PC1\text{-}S1\text{-}3}$ series with composites derived utilizing modelled bottom water temperature data supports this hypothesis, with significant coherence found between the proxy and model derived composites generated using all three strategies (Figure 3). These results strongly support the conclusions of recent marine proxy and pseudo-proxy based studies in the Northeast

Atlantic (Pyrina et al., 2017, Reynolds et al., 2017b) and the North Pacific (Black, 2009, Black et al., 2014) that multiple sclerochronological records can be used as part of a spatial network approach to investigate past marine variability.

Variability contained in the $\delta^{18}O_{PC1\text{-}S1}$ series is dominated by a gradual increase in $\delta^{18}O$ over the period from 1864 to ca. 1900 and a significant linear decrease in $\delta^{18}O$ over the 20th century (R=-0.74, P<0.001). The $\delta^{18}O_{PC1\text{-}S2\text{-}3}$ and $\delta^{18}O_{PC2\text{-}S1\text{-}2}$ series are dominated by multi-decadal scale variability and contain no significant long-term trends. In the case of the $\delta^{18}O_{PC1\text{-}S2\text{-}3}$ series such a result is to be expected as the PCA strategies employed broadly act as 50- and 30-year high pass filters respectively.

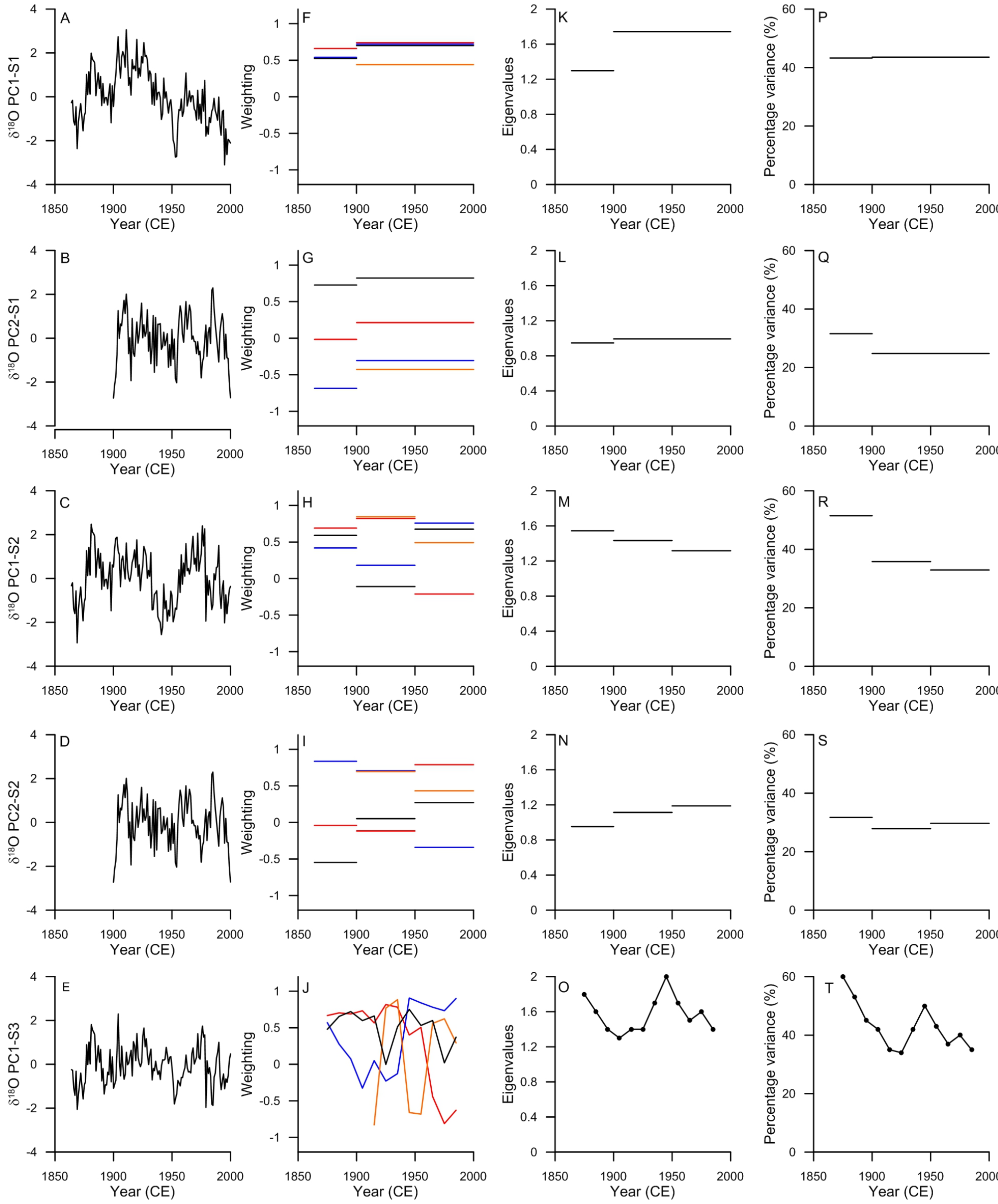

Figure 2: Comparison between PCs generated using the three strategies for conducting the PCA and relative weighting of the isotope series on the PC. A-E) The nested principal component outputs of the PCA using strategies 1 to 3 respectively. F-J) the relative weighting of the four independent $\delta^{18}O_{shell}$ series in each of the principal components. The red line represents the Scottish $\delta^{18}O_{shell}$ series, the orange represents the Norwegian $\delta^{18}O_{shell}$ series, the black line represents the Gulf of Maine $\delta^{18}O_{shell}$

series and the blue line the $\delta^{18}O_{shell}$ series from North Iceland. K-O) and P-T) show the Eigenvalue and percentage variance statistics for each of the $\delta^{18}O_{PC1-S1-3}$ and $\delta^{18}O_{PC2-S1-2}$ respectively.

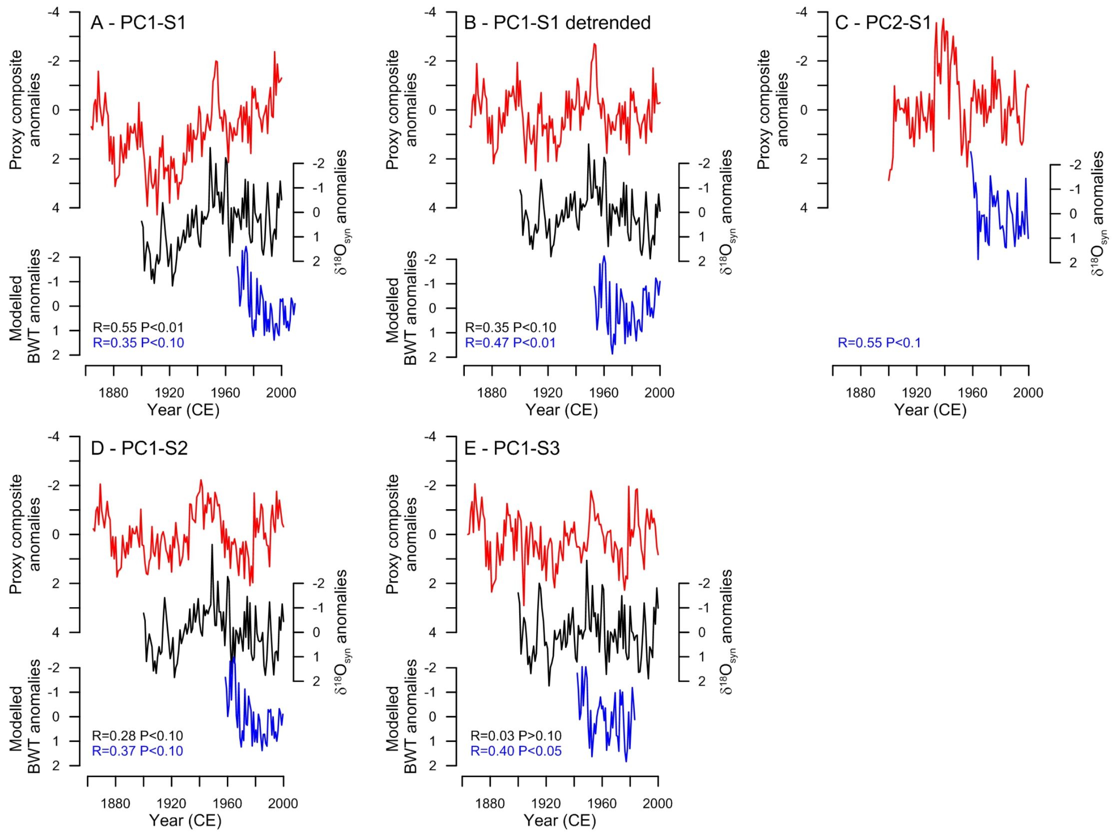

Figure 3: Comparison between the $\delta^{18}O_{PC-S1-3}$ series (red lines), $\delta^{18}O_{syn-PC1-S1-3}$ (black lines) and model (blue lines) derived composite series generated using the three PCA strategies. The corresponding correlation coefficients, and Monte Carlo derived probabilities, calculated between the proxy composites against the pseudo proxy and model derived composites are provided in blue and black text respectively. Correlations are calculated using the annually resolved data. No $\delta^{18}O_{syn-PC2-S1}$ series is plotted in panel C as the eigenvalues for this series are not significant (<1). Peak correlations between the $\delta^{18}O_{PC-S1-3}$ series and $\delta^{18}O_{syn-S1-S3}$ were obtained with zero year lag. However, peak correlations between the $\delta_{18OPC1S-3}$ series and Modelled data were obtained with the modelled data lagging the proxy composite by four to six years.

Environmental analyses and reconstruction skill

A range of significant relationships were identified using point correlation analyses between the proxy-based composites and gridded SST (HadISST1) and SSS (EN4 SSS) datasets across the North Atlantic region over the 20th century (Figure 4). In particular, the $\delta^{18}O_{PC1-S1}$ series contains significant coherence ($P<0.1$) with mean annual SSTs across the tropical North Atlantic from 0-40°N across the entire width of the North Atlantic basin and between variability contained in the $\delta^{18}O_{PC1-F}$ series, $\delta^{18}O_{PC1-S2-3}$ and $\delta^{18}O_{PC2-S1}$ series and variability in mean summer SSTs across regions of the North Atlantic broadly corresponding with the SPG (Figure 4 O, P and L). Quantitative examination of the point correlations, using linear regression analysis, show peak correlation between the $\delta^{18}O_{-PC1-S1}$ series and mean annual tropical Atlantic SSTs ($R=-0.64$ $P<0.05$; Figure 5) and between the $\delta^{18}O_{PC1-F}$, $\delta^{18}O_{PC1-S2-3}$ and $\delta^{18}O_{PC2-S1}$ series and mean summer SPG SSTs ($R=-0.31$, -0.34 and -0.39 respectively, $P<0.05$; Figures 4 and 5). The point correlations identified between the proxy based composite series and HadISSt1 data are consistent with the relationship observed between the $\delta^{18}O_{syn}$ based composites and the HadISST data

(Figure 4A). The strong coherence between the spatial distribution, and sign, of the point correlations calculated between the $\delta^{18}O_{PC1\text{-}S1}$ and $\delta^{18}O_{syn\text{-}PC1}$ series when correlated against gridded SST and SSS products (Figure 4) demonstrates that the variability extracted by the nested PCA and its sensitivity to basin-scale ocean dynamics is reproducible and, over the observational instrumental period, predictable using independent instrumental based records.

Examination of the point correlations generated between the $\delta^{18}O_{PC1\text{-}S1\text{-}3}$ and $\delta^{18}O_{PC1\text{-}F}$ (generated by high pass filtering the individual $\delta^{18}O_{shell}$ series; Figure 4 and Supplementary Figure S8) suggests differences in the spatial sensitivity of the proxy-based composites depending upon the timescale of variability contained in the composite series. For example, variability contained in the $\delta^{18}O_{PC1\text{-}S1}$ series, that incorporates both high and low frequency variability, contains a strong coherence with variability in the tropical North Atlantic. However, the $\delta^{18}O_{PC1\text{-}S2\text{-}3}$ and $\delta^{18}O_{PC1\text{-}F}$, that contain only sub-centennial scale variability, exhibit the strongest correlations with SST variability over the SPG region of the North Atlantic (Supplementary Figure S8). Given that both the $\delta^{18}O_{PC1\text{-}S2\text{-}3}$ and $\delta^{18}O_{PC1\text{-}F}$ series exhibit similar sensitivity to SPG SSTs suggests that the coherence is associated with the timescale of variability contained in the records and not associated with the methodologies used to generate the composite series. These analyses also highlight significant correlations with between the $\delta^{18}O_{PC1\text{-}F}$ composites and tropical Atlantic SSTs, however the correlations are weaker in nature than those identified in the analysis using the $\delta^{18}O_{PC1\text{-}S1}$ series. These analyses therefore suggest that the coherence between the $\delta^{18}O_{PC1\text{-}S1}$ and tropical North Atlantic SSTs is likely associated with longer timescale (centennial) variability, whilst the high frequency (sub-centennial) variability in the proxy composites is associated with SPG variability. This interpretation is supported by the examination of multiple linear regression analyses that highlights that SPG and tropical Atlantic SST variability can explain 41% ($P<0.001$) of the variability in the $\delta^{18}O_{PC1\text{-}S1}$ series. However, multiple linear regression analyses indicate that sub-centennial SPG and centennial tropical Atlantic SST variability can explain 61% of the variability in the $\delta^{18}O_{PC1\text{-}S1}$ series.

In addition to the strong coherence with SST variability, the point correlation analyses also identified significant coherence between the proxy based composite series and SSS variability (EN4 SSS) over the Norwegian Sea and along the coast of Nova Scotia respectively (Figure 4). The point correlations identified significant correlations ($P<0.1$) between the $\delta^{18}O_{PC1\text{-}S2}$ and $\delta^{18}O_{PC2\text{-}S1}$ series when correlated against mean winter SSS variability over the region of the North Atlantic between the northern British Isles and Iceland and across the Norwegian Sea (Figure 4K-L). Linear regression analyses between the $\delta^{18}O_{PC1\text{-}S2}$ and $\delta^{18}O_{PC2\text{-}S1}$ series and SSS data obtained from this region (57-67°N by 0-10°W) highlight the significant nature of the coherence between the $\delta^{18}O_{PC1\text{-}S2}$ and $\delta^{18}O_{PC2\text{-}S1}$ series and mean winter NAC SSS ($R=0.40$ and 0.42 respectively $P<0.05$; Figures 4 and 5).

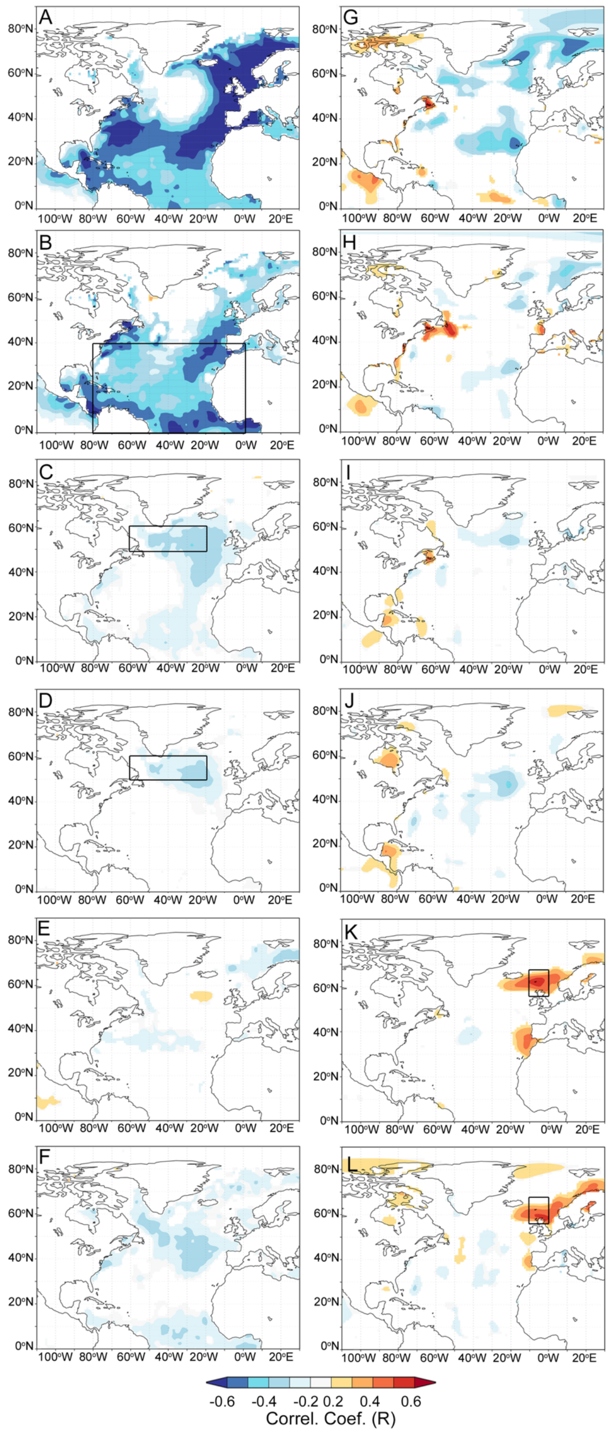

Figure 4: Point correlations calculated between the gridded SSTs (HadISST1 [panels A-F]) and SSSs (EN4 SSS [panels G-L]) correlated against A,G) the $\delta^{18}O_{syn}$ series; B,H) the $\delta^{18}O_{PC1-S1}$ series; C,I) the 100-year first order loess high pass filtered $\delta^{18}O_{PC1-S1}$ series; D,J) the $\delta^{18}O_{PC1-S3}$ series; E,K) the $\delta^{18}O_{PC2-S1}$ series; and F,L) the $\delta^{18}O_{PC1-S2}$ series. Point correlations calculated using annual resolution data over the entire 20th century and are significant at P<0.1 level. The correlations were conducted using KNMI Climate Explorer (https://climexp.knmi.nl/).

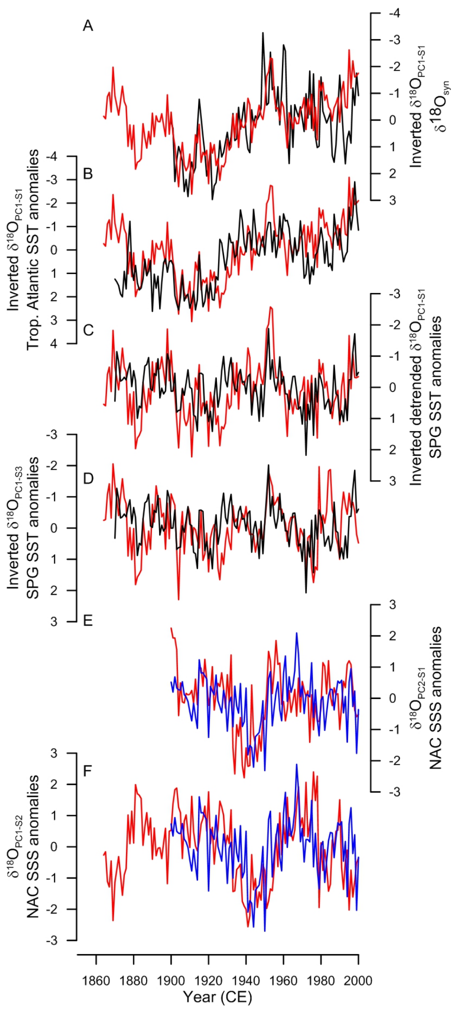

Figure 5: Comparison of the temporal and spatial sensitivity of the $\delta^{18}O_{PC1\text{-}S1\text{-}S3}$ and $\delta^{18}O_{PC2\text{-}S1}$ series against North Atlantic SSTs and SSS. A) The inverted $\delta^{18}O_{PC1\text{-}S1}$ (red line) and $\delta^{18}O_{syn\text{-}PC1}$ (black line) series. B) Tropical North Atlantic SST anomalies (black) plotted with the $\delta^{18}O_{PC1\text{-}S1}$ series (red line); C-D) SST anomalies from the SPG (black lines) plotted with the inverted C) detrended $\delta^{18}O_{PC1\text{-}S1}$ and D) the $\delta^{18}O_{PC1\text{-}S3}$ series respectively (red lines). E-F) SSS anomalies from the NAC (blue lines) plotted with E) the $\delta^{18}O_{PC2\text{-}S1}$ and F) the $\delta^{18}O_{PC1\text{-}S2}$ series. The instrumental data plotted in panels B-F are calculated as the mean SST/SSS of the data derived from the HadISST1 and EN4 SSS datasets over the areas highlighted by the black box inserts in Figure 4 panels B-D, K and L respectively.

The correlations between the hypothetical proxy network, constructed using different numbers of theoretical proxy records (based on observational SST data) from the continental margins and across the North Atlantic Ocean, against mean North Atlantic SSTs indicates that increasing the number of proxy records would increase the sensitivity of the resulting composite series to wider North Atlantic SSTs. The correlation increases from R=0.68 (P<0.001), when using the SST_{PC1} series generated using the four sampling location used in this study, up to R=0.81 (P<0.001) when using 14 shelf sea sampling locations. The correlation increases further to R=0.93 (P<0.001) if these 14 shelf sea records could be integrated with records from the central North Atlantic region. As no proxy record has absolute skill at reconstructing local SSTs these values are an overestimate of the likely ability of the proxy-based network to reconstruct North Atlantic North Atlantic SSTs. However, whilst the precise degree of coherence may vary, these analyses do demonstrate that increasing the number of independent shelf sea sclerochronological records included in our network would be beneficial and enhance our ability to skillfully reconstruct open ocean variability. At present there are no annually resolved surface ocean proxy records available from the central North Atlantic Ocean that could be included in the network, but there are numerous high-resolution sediment core proxy records that could potentially be utilized. Whilst integrating mixed archive proxy records with variable age and proxy uncertainties would inherently add complexity to the construction of a spatial network (Cunningham et al., 2013; McGregor et al., 2015), our hypothetical considerations suggest integrating records from this region would potentially increase the ability of the network to reconstruct past central North Atlantic Ocean variability, especially at decadal to multidecadal timescales.

The split calibration-verification methodology quantitatively evaluated the skill of each of the proxy composite series at reconstructing the selected target parameter. The resulting RE and CE statistics were positive for each of the proxy-based reconstructions of the respective target parameters (Table 1). The RE and CE statistics are significant if greater than zero indicating that the corresponding reconstructions contain significant skill at reconstructing the target parameters. These results indicate that the calibrated $\delta^{18}O_{PC1-S1}$ series provides a skillful reconstruction of tropical North Atlantic SSTs, the $\delta^{18}O_{PC1-S2}$ series skillful reconstructions of NAC SSTs and SPG SSTs, the $\delta^{18}O_{PC1-S2}$ series skillful reconstructions of mean summer SPG SSTs and the $\delta^{18}O_{PC2-S1}$ series a skillful reconstruction of winter NAC SSTs (Figure 6).

Table 1: Calibration and verification statistics calculated between the $\delta^{18}O_{PC1-S1-3}$ and $\delta^{18}O_{PC2-S1}$ series and North Atlantic SSTs and SSS. The correlation statistics are calculated over the entire 20th century. The correlation confidents, reduction of error (RE) and coefficient of efficiency (CE) statistics are calculated using Ebisuzaki Monte Carlo methodology using 1000 reanalyzes. The RE and CE statistics are significant if ≥0. All correlations shown in the table are significant at a level of $P<0.05$.

Proxy	**Target parameter**	**R**	**R^2**	**RE**	**CE**
$\delta^{18}O_{PC1-S1}$	Annual Tropical Atlantic SSTs	-0.64	0.41	0.52	0.14
$\delta^{18}O_{PC1-S1}$ detrended	Summer SPG SSTs	-0.39	0.15	0.08	0.08
$\delta^{18}O_{PC1-S3}$	Summer SPG SSTs	-0.34	0.12	0.12	0.12
$\delta^{18}O_{PC1-S2}$	Summer SPG SSTs	-0.31	0.10	0.08	0.07
$\delta^{18}O_{PC2-S1}$	Winter NAC SSS	0.42	0.18	0.12	0.11
$\delta^{18}O_{PC1-S2}$	Winter NAC SSS	0.40	0.16	0.18	0.17

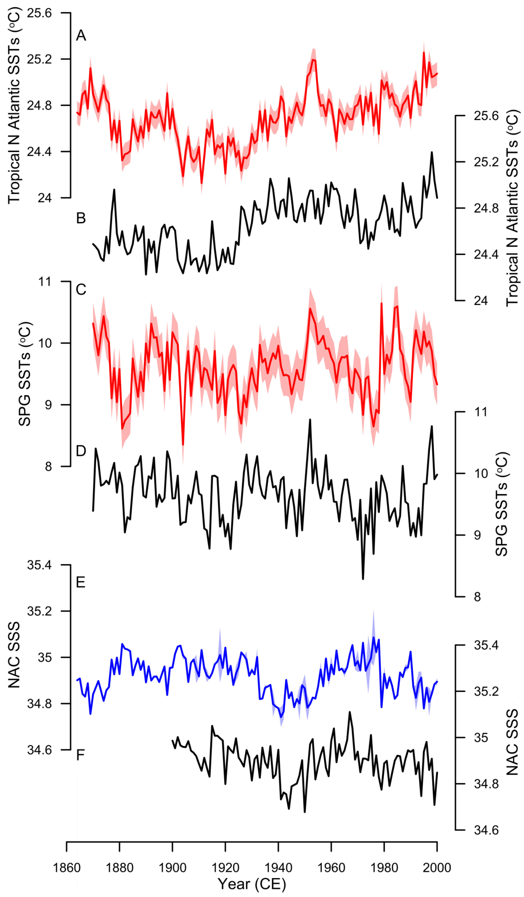

Figure 6: A-B) Reconstructed (red line) and observed (black line) tropical North Atlantic SSTs respectively. C-D) Reconstructed (red line) and observed SPG SSTs respectively. E-F) Reconstructed (blue line) and observed (black line) winter SSS in the NAC. The shaded red and blue areas around plots A, C and E represent the two times MSE uncertainty envelope.

Sensitivity to ocean and atmospheric circulation

The identification of significant correlations between the $\delta^{18}O_{PC1\text{-}S1\text{-}3}$ series and tropical North Atlantic SSTs, SPG SSTs and NAC SSSs highlights the significance of the interplay between the tropical and subpolar North Atlantic dynamics in modulating environmental variability across the continental shelf seas of the North Atlantic Ocean. Given the time it takes for signals to propagate northwards through the surface ocean from the equatorial Atlantic to the subpolar latitudes (Getzlaff et al., 2005), these results suggest that both marine and atmospheric circulation patterns are playing a role in driving the common variability across the four independent $\delta^{18}O_{shell}$ series.

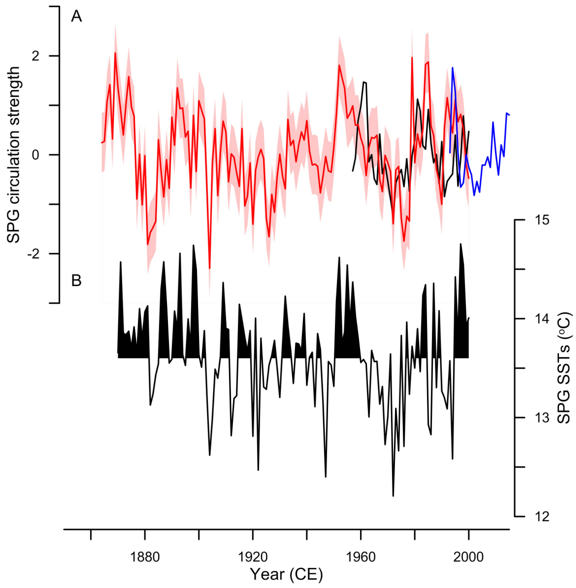

Figure 7: A) Comparison between the $\delta^{18}O_{PC1\text{-}S3}$ series (red line and shaded red envelope) and the Marsh et al., (2017) ESC annual index (black line) and the Hatun et al., (2005) SPG index (blue line). B) Mean annual SPG HadISST1 SSTs (black line) with years containing SSTs greater than the mean shaded in black.

The linear regression analyses between the linear detrended $\delta^{18}O_{PC1\text{-}S1\text{-}S3}$ series and the ESC annual index (Marsh et al., 2017) identified a range of correlations ($\delta^{18}O_{PC1\text{-}S1}$ R=-0.14, P>0.1; $\delta^{18}O_{PC1\text{-}S2}$ R=-0.30, P=0.06; $\delta^{18}O_{PC1\text{-}S3}$ R>-0.1 P>0.1). Examination of the correlations between the linear detrended five year first order loess low pass filtered linear detrended series demonstrates a marked increase in the strength of the correlations ($\delta^{18}O_{PC1\text{-}S1}$ R=-0.27, P>0.1; $\delta^{18}O_{PC1\text{-}S2}$ R=-0.62, P<0.01; $\delta^{18}O_{PC1\text{-}S3}$ R=-0.57 P<0.05). The identification of significant correlations between the $\delta^{18}O_{PC1\text{-}S3}$ series and the ESC annual index, most notably using the 5-year smoothed linear detrended data ($\delta^{18}O_{PC1\text{-}S2}$ and $\delta^{18}O_{PC1\text{-}S3}$), strongly suggests that the variability captured by the proxy composite series is, in part, associated with the advection of warm and salty waters through the North Atlantic Ocean surface circulation. These analyses indicate that periods of enhanced (reduced) ESC strength (by extension SPG strength, Hatun et al., 2005) coincide with periods of warm (cold) SPG SSTs and lower (higher) $\delta^{18}O_{PC1\text{-}S2\text{-}3}$ values (Figure 7). The relatively weak coherence with inter-annual variability, however, suggests that other mechanisms mask the variability on inter-annual timescales.

The point correlation analyses between the proxy composite series against gridded SLP and zonal wind stress data yielded a range of significant correlations (P<0.1; Supplementary Figure S10). A dipole pattern of positive and negative correlations was identified over the tropical and polar North Atlantic regions respectively between the proxy composite series and SLPs using both linear detrended and non- detrended datasets (Supplementary Figure S10). Similarly, a dipole pattern of correlations over the tropical and subpolar regions of the North Atlantic was identified in the correlations between the composite proxy series and zonal wind stress, also using both linear detrended and none detrended data (Supplementary Figure S10). The identification of significant correlations between the proxy series and both gridded SLP and zonal wind stress data sets strongly indicates that atmospheric circulation patterns play a role in propagating the tropical Atlantic and SPG temperature signals towards the coastal regions of the North Atlantic. These analyses are therefore in agreement with the proposed mechanisms and forcings identified by previous modelling efforts (e.g. Marsh et al., 2015). The sign, spatial distribution and seasonality of the correlations between the proxy series and SLPs is characteristic of the dipole pressure gradient associated with the wNAO, with significant positive and negative correlations occurring during winter over the tropical and polar regions of the North Atlantic respectively (Supplementary Figure S10).

Conclusion

Although there are presently only a few individual $\delta^{18}O_{shell}$ records that span multi-centennial to millennial timespans, these analyses highlight that applying nested PCA to a suite of sclerochronological $\delta^{18}O_{shell}$ records, from across the North Atlantic Ocean region, can facilitate the quantitative reconstruction of basin scale ocean dynamics. Supplementing the current network of $\delta^{18}O_{shell}$ records with additional sclerochronological and well dated high resolution sediment core proxy records of surface ocean variability will further enhance our ability to quantitatively investigate past ocean dynamics. Whilst the application of terrestrial proxy-derived marine reconstructions (e.g. Gray, 2004, Mann et al., 2014, Rahmstorf et al., 2015) may currently provide significantly longer reconstructions, they lack independence from reconstructions of atmospheric dynamics (being based on the same tree ring series). This lack of independence between the marine and atmospheric reconstructions restricts our ability to analyze and quantify the influence that marine variability has on atmospheric climate variability. The development of independent marine reconstructions is therefore essential for the robust assessment of the past influence of marine variability on the climate system. The continued development of quantitative reconstructions of past marine variability will have a profound influence on our ability to validate numerical climate models and to help constrain uncertainties in near-term decadal scale climate predictions.

Acknowledgements

This work was supported in part by the Natural Environment Research Council funded Climate of the Last Millennium Project (Project No. NE/N001176/1) and National Science Foundation (grant 1417766 to ADW). The authors would like to thanks the two anonymous reviewers for their constructive reviews that significantly improved this manuscript.

Data availability

The four $\delta^{18}O_{shell}$ records analyzed in this study are publicly available at https://www.ncdc.noaa.gov/data-access/paleoclimatology-data/datasets

The instrumental data used in this study are available at http://climexp.knmi.nl/

References

Berx, B. and M. R. Payne (2017). The sub-polar gyre index - a community data set for application in fisheries and environment research. *Earth System Science Data,* 9**,** 259-266.

Black, B. A. (2009). Climate-driven synchrony across tree, bivalve, and rockfish growth-increment chronologies of the northeast pacific. *Mar Ecol Prog Ser,* 378**,** 37-46.

Black, B. A., W. J. Sydeman, D. C. Frank, D. Griffin, D. W. Stahle, M. Garcia-Reyes, R. R. Rykaczewski, S. J. Bograd and W. T. Peterson (2014). Climate change. Six centuries of variability and extremes in a coupled marine-terrestrial ecosystem. *Science,* 345**,** 1498-502.

Bryden, H. L., H. R. Longworth and S. A. Cunningham (2005). Slowing of the atlantic meridional overturning circulation at 25 degrees n. *Nature,* 438**,** 655-7.

Cage, A. G. and W. E. N. Austin (2010). Marine climate variability during the last millennium: The loch sunart record, scotland, uk. *Quaternary Science Reviews,* 29**,** 1633-1647.

Cunningham, L. K., W. E. Austin, K. L. Knudsen, J. Eiriksson, J. D. Scourse, A. D. Wanamaker, P. G. Butler, A. G. Cage, T. Richter, K. Husum, M. Hald, C. Andersson, E. Zorita, H. W. Linderholm, B. E. Gunnarson, M. A. Sicre, H. P. Sejrup, H. Jiang and R. J. Wilson (2013). Reconstructions of surface ocean conditions from the northeast atlantic and nordic seas during the last millennium. *The Holocene,* 23, 921-935.

Cunningham, S. A., T. Kanzow, D. Rayner, M. O. Baringer, W. E. Johns, J. Marotzke, H. R. Longworth, E. M. Grant, J. J. M. Hirschi, L. M. Beal, C. S. Meinen and H. L. Bryden (2007). Temporal variability of the atlantic meridional overturning circulation at 26.5 degrees n. *Science,* 317, 935-938.

Drijfhout, S., G. J. Van Oldenborgh and A. Cimatoribus (2012). Is a decline of amoc causing the warming hole above the north atlantic in observed and modeled warming patterns? *J Clim,* 25, 8373-8379.

Ebisuzaki, W. (1997). A method to estimate the statistical significance of a correlation when the data are serially correlated. *J Clim,* 10, 2147-2153.

Foukal, N. P. and M. S. Lozier (2017). Assessing variability in the size and strength of the north atlantic subpolar gyre. *Journal of Geophysical Research-Oceans,* 122, 6295-6308.

Freeman, E., S. D. Woodruff, S. J. Worley, S. J. Lubker, E. C. Kent, W. E. Angel, D. I. Berry, P. Brohan, R. Eastman, L. Gates, W. Gloeden, Z. H. Ji, J. Lawrimore, N. A. Rayner, G. Rosenhagen and S. R. Smith (2017). Icoads release 3.0: A major update to the historical marine climate record. *International Journal of Climatology,* 37, 2211-2232

Getzlaff, J., Boning, C. W., Eden, C. & Biastoch, A. 2005. Signal propagation related to the North Atlantic overturning. *Geophysical Research Letters,* 32.

Good, S. A., M. J. Martin and N. A. Rayner (2013). En4: Quality controlled ocean temperature and salinity profiles and monthly objective analyses with uncertainty estimates. *Journal of Geophysical Research-Oceans,* 118, 6704-6716.

Gray, S. T. (2004). A tree-ring based reconstruction of the atlantic multidecadal oscillation since 1567 a.D. *Geophys Res Lett,* 31.

Hakkinen, S. and P. B. Rhines (2004). Decline of subpolar north atlantic circulation during the 1990s. *Science,* 304, 555-559.

Hatun, H., A. B. Sando, H. Drange, B. Hansen and H. Valdimarsson (2005). Influence of the atlantic subpolar gyre on the thermohaline circulation. *Science,* 309, 1841-1844.

Huthnance, J. M. (1984). Slope currents and jebar. *J Phys Oceanogr,* 14, 795-810.

Kennedy, J. J., N. A. Rayner, R. O. Smith, D. E. Parker and M. Saunby (2011). Reassessing biases and other uncertainties in sea surface temperature observations measured in situ since 1850: 2. Biases and homogenization. *Journal of Geophysical Research-Atmospheres,* 116.

Macias-Fauria, M., A. Grinsted, S. Helama and J. Holopainen (2012). Persistence matters: Estimation of the statistical significance of paleoclimatic reconstruction statistics from autocorrelated time series. *Dendrochronologia,* 30, 179-187.

Mann, M. E., B. A. Steinman and S. K. Miller (2014). On forced temperature changes, internal variability, and the amo. *Geophys Res Lett,* 41, 3211-3219.

Mann, M. E., Z. Zhang, S. Rutherford, R. S. Bradley, M. K. Hughes, D. Shindell, C. Ammann, G. Faluvegi and F. Ni (2009). Global signatures and dynamical origins of the little ice age and medieval climate anomaly. *Science,* 326, 1256-1260.

Marsh, R., I. D. Haigh, S. A. Cunningham, M. E. Inall, M. Porter and B. I. Moat (2017). Large-scale forcing of the european slope current and associated inflows to the north sea. *Ocean Sci,* 13.

Marsh, R., A. E. Hickman and J. Sharples (2015). S2p3-r (v1.0): A framework for efficient regional modelling of physical and biological structures and processes in shelf seas. *Geoscientific Model Development,* 8, 3163-3178.

Marshall, J., Y. Kushner, D. Battisti, P. Chang, A. Czaja, R. Dickson, J. Hurrell, M. Mccartney, R. Saravanan and M. Visbeck (2001). North atlantic climate variability: Phenomena, impacts and mechanisms. *International Journal of Climatology,* 21, 1863-1898.

Marzocchi, A., J. J. M. Hirschi, N. P. Holliday, S. A. Cunningham, A. T. Blaker and A. C. Coward (2015). The north atlantic subpolar circulation in an eddy-resolving global ocean model. *J Mar Syst,* 142**,** 126-143.

Mcgregor, H. V., M. N. Evans, H. Goosse, G. Leduc, B. Martrat, J. A. Addison, P. G. Mortyn, D. W. Oppo, M. S. Seidenkrantz, M. A. Sicre, S. J. Phipps, K. Selvaraj, K. Thirumalai, H. L. Filipsson and V. Ersek (2015). Robust global ocean cooling trend for the pre-industrial common era. *Nature Geoscience,* 8**,** 671-+.

Mette, M. J., A. D. Wanamaker, Jr., M. L. Carroll, W. G. Ambrose, Jr. and M. J. Retelle (2016). Linking large-scale climate variability with arctica islandica shell growth and geochemistry in northern norway. *Limnol Oceanogr,* 61**,** 748-764.

Moberg, A., D. M. Sonechkin, K. Holmgren, N. M. Datsenko and W. Karlen (2005). Highly variable northern hemisphere temperatures reconstructed from low- and high-resolution proxy data. *Nature,* 433**,** 613-617.

Moffa-Sánchez, P., A. Born, I. R. Hall, D. J. R. Thornalley and S. Barker (2014). Solar forcing of north atlantic surface temperature and salinity over the past millennium. *Nature Geoscience,* 7**,** 275-278.

Moffa Sanchez, P. and I. Hall (2017). North atlantic variability and its links to european climate over the last 3000 years. *Nature Communications,* 8.

Moreno-Chamarro, E., D. Zanchettin, K. Lohmann, J. Luterbacher and J. H. Jungclaus (2017). Winter amplification of the european little ice age cooling by the subpolar gyre. *Scientific Reports,* 7.

North, G. R., Biondi, F., Bloomfield, P., Christy, J.R., Cuffey, K.M., Dickinson, R.E., Druffel, E.R.M., Nychka, D., Otto-Bliesner, B., Roberts, N., Turekian, K.K., Wallace, J.M. 2000. *Surface temperature reconstructions for the last 2,000 years.*, The National Academies Press, New York.

Pyrina, M., S. Wagner and E. Zorita (2017). Pseudo-proxy evaluation of climate field reconstruction methods of north atlantic climate based on an annually resolved marine proxy network. *Climate of the Past,* 13**,** 1339–1354.

Rahmstorf, S., J. E. Box, G. Feulner, M. E. Mann, A. Robinson, S. Rutherford and S. E. J. (2015). Exceptional twentieth-century slowdown in atlantic ocean overturning circulation. *Nature Climate Change*.

Rayner, N. A., D. E. Parker, E. B. Horton, C. K. Folland, L. V. Alexander, D. P. Rowell, E. C. Kent and A. Kaplan (2003). Global analyses of sea surface temperature, sea ice, and night marine air temperature since the late nineteenth century. *Journal of Geophysical Research-Atmospheres,* 108.

Reynolds, D. J., I. R. Hall, S. Slater, J. D. Scourse, P. R. Halloran and M. D. J. Sayer (2017a). Reconstructing past seasonal to multi-centennial scale variability in the ne atlantic ocean using the long-lived marine bivalve mollusc glycymeris glycymeris. *Paleocanography*.

Reynolds, D. J., C. A. Richardson, J. D. Scourse, P. G. Butler, P. Hollyman, A. Roman-Gonzalez and I. R. Hall (2017b). Reconstructing north atlantic marine climate variability using an absolutely-dated sclerochronological network. *Palaeogeography Palaeoclimatology Palaeoecology,* 465**,** 333-346.

Reynolds, D. J., J. D. Scourse, P. R. Halloran, A. J. Nederbragt, A. D. Wanamaker, P. G. Butler, C. A. Richardson, J. Heinemeier, J. Eiriksson, K. L. Knudsen and I. R. Hall (2016). Annually resolved north atlantic marine climate over the last millennium. *Nature Communications,* 7.

Smeed, D., G. Mccarthy, D. Rayner, B. I. Moat, W. E. Johns, M. O. Baringer and C. S. Meinen (2016). Atlantic meridional overturning circulation observed by the rapid-mocha-wbts (rapid-meridional overturning circulation and heatflux array-western boundary time series) array at 26n from 2004 to 2015. *British Oceanographic Data Centre - Natural Environment Research Council, UK.*

Smeed, D. A., S. A. Josey, C. Beaulieu, W. E. Johns, B. I. Moat, E. Frajka-Williams, D. Rayner, C. S. Meinen, M. O. Baringer, H. L. Bryden and G. D. Mccarthy (2018). The north atlantic ocean is in a state of reduced overturning. *Geophys Res Lett,* 45**,** 1527-1533.

Smeed, D. A., G. D. Mccarthy, S. A. Cunningham, E. Frajka-Williams, D. Rayner, W. E. Johns, C. S. Meinen, M. O. Baringer, B. I. Moat, A. Duchez and H. L. Bryden (2014). Observed decline of the atlantic meridional overturning circulation 2004-2012. *Ocean Sci,* 10**,** 29-38.

Smith, L. M., J. T. Andrews, I. S. Castañeda, G. B. Kristjánsdóttir, A. E. Jennings and Á. E. Sveinbjörnsdóttir (2005). Temperature reconstructions for sw and n iceland waters over the last 10calka based on δ18o records from planktic and benthic foraminifera. *Quaternary Science Reviews,* 24**,** 1723-1740.

Smith, T. M., R. W. Reynolds, T. C. Peterson and J. Lawrimore (2008). Improvements to noaa's historical merged land-ocean surface temperature analysis (1880-2006). *J Clim,* 21**,** 2283-2296.

Thirumalai, K., T. M. Quinn, Y. Okumura, J. N. Richey, J. W. Partin, R. Z. Poore and E. Moreno-Chamarro (2018). Pronounced centennial-scale atlantic ocean climate variability correlated with western hemisphere hydroclimate. *Nature Communications,* 9.

Trenberth, K. E. and D. A. Paolino (1980). The northern hemisphere sea-level pressure data set - trends, errors and discontinuities. *Monthly Weather Review,* 108**,** 855-872.

Trouet, V. and G. J. Van Oldenborgh (2013). Climate explorer: A web-based research tool for high-resolution paleoclimatology. *Tree-Ring Research,* 69**,** 3-13.

Wainer, I., J. Servain and G. Clauzet (2008). Is the decadal variability in the tropical atlantic a precursor to the nao? *Ann Geophys,* 26**,** 4075-4080.

Wanamaker, A. D., Jr., P. G. Butler, J. D. Scourse, J. Heinemeier, J. Eiriksson, K. L. Knudsen and C. A. Richardson (2012). Surface changes in the north atlantic meridional overturning circulation during the last millennium. *Nat Commun,* 3**,** 899.

Wanamaker, A. D., Jr., K. J. Kreutz, B. R. Schoene and D. S. Introne (2011). Gulf of maine shells reveal changes in seawater temperature seasonality during the medieval climate anomaly and the little ice age. *Palaeogeography Palaeoclimatology Palaeoecology,* 302**,** 43-51.

Wanamaker, A. D., K. J. Kreutz, B. R. Schoene, N. Pettigrew, H. W. Borns, D. S. Introne, D. Belknap, K. A. Maasch and S. Feindel (2008). Coupled north atlantic slope water forcing on gulf of maine temperatures over the past millennium. *Climate Dynamics,* 31**,** 183-194.

Whitney, N. M., A. D. Wanamaker, K. J. Kreutz and D. S. Introne (2017). Spatial and temporal variability in the delta o-18(w) and salinity compositions of gulf of maine coastal surface waters. *Cont Shelf Res,* 137**,** 163-171.

Wilson, R., K. Anchukaitis, K. R. Briffa, U. Buentgen, E. Cook, R. D'arrigo, N. Davi, J. Esper, D. Frank, B. Gunnarson, G. Hegerl, S. Helama, S. Klesse, P. J. Krusic, H. W. Linderholm, V. Myglan, T. J. Osborn, M. Rydval, L. Schneider, A. Schurer, G. Wiles, P. Zhang and E. Zorita (2016). Last millennium northern hemisphere summer temperatures from tree rings: Part i: The long term context. *Quaternary Science Reviews,* 134**,** 1-18.

Wilson, R., E. Cook, R. D'arrigo, N. Riedwyl, M. N. Evans, A. Tudhope and R. Allan (2010). Reconstructing enso: The influence of method, proxy data, climate forcing and teleconnections. *Journal of Quaternary Science,* 25**,** 62-78.

Xie, S. P. and J. A. Carton (2004). Tropical atlantic variability: Patterns, mechanisms, and impacts. *Earth's Climate: the Ocean-Atmosphere Interaction,* 147**,** 121-142.

Zhang, R. (2008). Coherent surface-subsurface fingerprint of the atlantic meridional overturning circulation. *Geophys Res Lett,* 35.